

# Cycling of Rational Hybridization Chain Reaction To Enable Enzyme-Free DNA-Based Clinical Diagnosis

Gaolian Xu,<sup>†,‡</sup> Hang Zhao,<sup>‡,§</sup> Julien Reboud,<sup>‡</sup> and Jonathan M. Cooper<sup>\*,‡,§</sup>

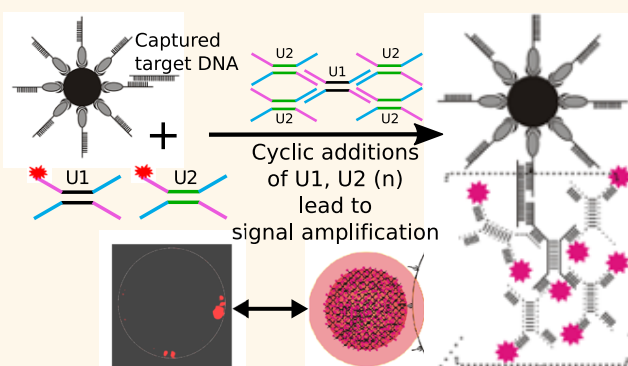
<sup>†</sup>Nano Biomedical Research Centre, School of Biomedical Engineering, Shanghai Jiao Tong University, Shanghai 200030, P. R. China

<sup>‡</sup>Division of Biomedical Engineering, School of Engineering, University of Glasgow, Glasgow G12 8LT, U.K.

## S Supporting Information

**ABSTRACT:** In order to combat the growing threat of global infectious diseases, there is a need for rapid diagnostic technologies that are sensitive and that can provide species specific information (as might be needed to direct therapy as resistant strains of microbes emerge). Here, we present a convenient, enzyme-free amplification mechanism for a rational hybridization chain reaction, which is implemented in a simple format for isothermal amplification and sensing, applied to the DNA-based diagnosis of hepatitis B virus (HBV) in 54 patients. During the cycled amplification process, DNA monomers self-assemble in an organized and controllable way only when a specific target HBV sequence is present. This mechanism is confirmed using super-resolution stochastic optical reconstruction microscopy. The enabled format is designed in a manner analogous to an enzyme-linked immunosorbent assay, generating colored products with distinct tonality and with a limit of detection of ca. five copies/reaction. This routine assay also showed excellent sensitivity (>97%) in clinical samples demonstrating the potential of this convenient, low cost, enzyme-free method for use in low resource settings.

**KEYWORDS:** DNA self-assembly, hybridization chain reaction, cycling, enzyme-free, diagnostic, HBV



The sensitive and specific detection of nucleic acids is important in a wide range of clinical diagnostic analyses. Although DNA biosensors have previously been developed,<sup>1</sup> currently their implementation often relies on the enzymatic amplification of the target DNA. This can be achieved using either thermal cycling (e.g., polymer chain reaction, PCR), isothermal amplification methods, such as loop-mediated isothermal amplification (LAMP)<sup>2</sup> or cross-priming amplification (CPA),<sup>3</sup> for example. Many of these enzyme-mediated assays have been constrained in their use, requiring well-resourced settings with well-controlled environmental conditions (for enzyme storage) as well as the need for complex sample purification steps (to avoid reaction inhibitors present in samples).

To overcome these limitations, isothermal, enzyme-free methods have been developed, based on specific DNA hybridization, which amplify the biochemical signal.<sup>4</sup> As a general scheme, the presence of target DNA (from bacteria, for example) leads to the opening of DNA hairpin structures to create a chain reaction involving many hairpin openings, resulting in multiple hybridizations. Such cascades lead to the

formation of a large DNA complex, which can then be easily detected, either optically or using label-free sensing.<sup>5–9</sup> This chain reaction and, thus, the molecular weight/size of the product (as the amplified signal) have proven to be difficult to control, limiting the opportunities to develop high sensitivity and quantitative assays. Consequently, enzymatic mediated methods, such as PCR, remain the gold standard for DNA amplification and sensing, providing quantitative and controllable amplification, albeit in well-controlled environmental conditions.<sup>10,11</sup>

We now show a different class of HCR assay which combines the advantages of controlled amplification with hybridization (as the fundamental principles of an enzyme-free biochemical reaction) in order to develop a quantitative and sensitive DNA amplification technique. The technique is self-limiting, as the amplification is sustained only until reactants become kinetically depleted.

Received: April 27, 2018

Accepted: July 2, 2018

Published: July 2, 2018

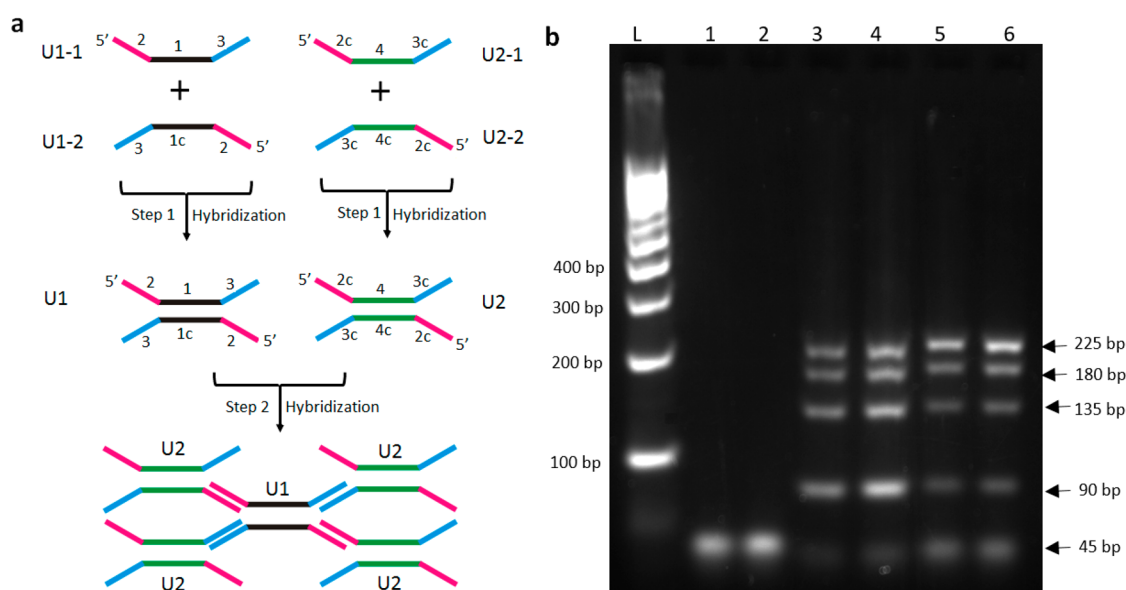


**Figure 1.** Reaction principle of db DNA-based rational HCR. (a) Schematic illustration of synthesis and inter-reaction of db DNA units. Two starting oligonucleotides (U1-1/U1-2 or U2-1/U2-2) possess the same sticky ends at 3' and 5' ends, as well as complementary midsequence segments, as indicated. For the process starting from U1 (left), the db DNA units (U1 or U2) hybridize (step 1). Similarly, the DNA synthesis process can also begin from U2 (right). The formed db DNA units (U2) can be combined to U1 during the rational HCR process (step 2), due to their exposed complementary sticky ends. Thus, by addition of U2 and U1 successively and repeatedly, these two units can bind to each other leading to an exponential growth of a packed complex 3D DNA structure (step n); (b) Evaluation of the product of db DNA-based rational HCR using gel electrophoresis. L lane was 100 bp ladder, lane 1 and 2 were U1 and U2, Lanes 3 and 4 were the hybridized products of U1 and U2 with stoichiometry ratio at 5:1 (and 1:5, respectively), and Lanes 5 and 6 were the product of stoichiometry ratio at 20:1 (and 1:20, respectively), the unit with a low concentration was kept at 0.1  $\mu\text{M}$ . Bands from 90 to 225 bp (from lane 3 to 6) illustrate the expected products ratios, which are different to those from the smallest units (lane 1/2). For this concentration of single units, larger products are not formed efficiently (evidence of limited formation is shown by smears in the large sizes), since the single units become depleted as the reaction progresses.

## RESULTS AND DISCUSSION

**Reaction Mechanism.** The proposed rational HCR is based on two primer dumbbell-shaped DNA (db DNA) structures (U1 and U2), capable of binding to each other stoichiometrically (one unit of each can bind to 4 units of the other, Figure 1a), thus providing the potential for an exponential growth. The primer dumbbells are formed by two starting oligonucleotides (U1-1/U1-2 and U2-1/U2-2) with a complementary nucleotide matching in their midsequence (1/1c of U1 and 4/4c of U2). There are also two exposed "sticky" ends, each complementary to the other (e.g., 2 of U1 is complementary to 2c of U2). At each cycle, one unit (e.g., U1) serves as the template for the hybridization with a number of the other unit (e.g., U2). Once hybridization is complete, the second unit (e.g., U2) is removed from the reaction volume and replaced with the first unit (e.g., U1), which can then hybridize with the product of the previous cycle.

The amplification factor and, thus, the molecular weight of the amplicon at each cycle are linked to the number of units that can bind to the product of the previous cycle, between 1 and 4 (which is itself dependent on the concentration ratios between the 2 units, Figure 1b). By analogy to the PCR cycle, the rate of amplification reaches a plateau as the concentration of available primers for the reaction decreases, and the kinetics of the reaction become rate-limiting.

We confirmed the relationship between the molecular weight of the amplicon after the first cycle and the stoichiometry ratios of the db DNA primers, using gel electrophoresis. Figure 1b shows the db DNA units (U1 and

U2) alone (45 bp, lanes 1–2) and after having been mixed in a ratio of 1:5 (lanes 3–4) and 1:20 (lanes 5–6). The reaction forms stable structures with 2 db DNA and 3, 4, and 5 db DNA together. As the stoichiometric ratio decreases, the amount of the larger complexes increases at the expense of the smaller ones. For example, the intensity of the band at 225 bp (5 dbDNA) is similar (unitary) to the band at 90 bp (2 dbDNA) at a ratio of 1:5 but is much higher (double) at a ratio of 1:20. Theoretically, the first step of the reaction should proceed at maximal efficiency (or coverage) with a ratio of 1:4, where all U1 binds to 4 U2 (Figure 1a); however, due to mass transfer and competing hybridizations, a range of constructs of different sizes are formed, while larger sizes are favored by smaller ratios. In order to demonstrate that this rational HCR DNA amplification system forms large, packed DNA nanostructures as predicted, we used a system where a single dumbbell DNA structure can self-hybridize (Figure S1a) at the same stoichiometry as that of the 2 db structure, i.e., at a ratio of 1:4. The product of this single db DNA-mediated HCR was evaluated using gel electrophoresis (Figure S1b), showing bands of increasing sizes, corresponding to increasing numbers of unit db DNA bound together, as well as products with a much larger size (as a smear).

**Reaction Cycling.** As discussed, the control of the rate of reaction is dependent upon the stoichiometric ratio between the two db DNA primers, one being in excess to the other, in order to build a structure based on a 1:4 complex. To then continue amplification, this excess needs to be reversed. Here, we show that this can be implemented conveniently through the immobilization of the appropriate reagents on beads with a

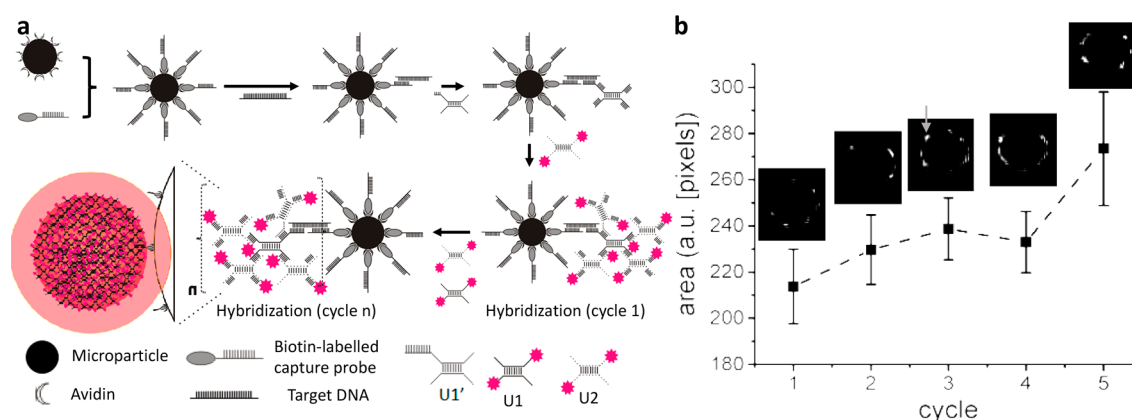


**Figure 2.** Microbead-based DNA detection: (a) Schematic drawing of db DNA-based rational HCR for signal amplification of target DNA from magnetic microbeads. Briefly, biotin-labeled capture probes were immobilized onto avidin-functionalized microbeads. Target DNA was then captured by these specific microbeads. The detection probe links to U1' and is also complementary to a second part of the target DNA and thus enabled U1 to bind to the surface of microbeads (see Table S1 for details). Fluorescence-labeled db DNA units were successively added to amplify the signal, forming larger constructs as the reactions proceeds. A washing step is necessary after each hybridization step to remove the excess db DNA units. (b) Fluorescence signal of microbeads at different cycles, imaged by super-resolution stochastic optical reconstruction microscopy (STORM) (the images' contrast and brightness were modified for ease of presentation) and analyzed using segmentation (see Figure S4 for an example of the process), showing the average area of a fluorescent spot (measured in pixels) for at least 10 beads for each cycle of washing and addition of reagent. All beads are 5  $\mu\text{m}$  in diameter.

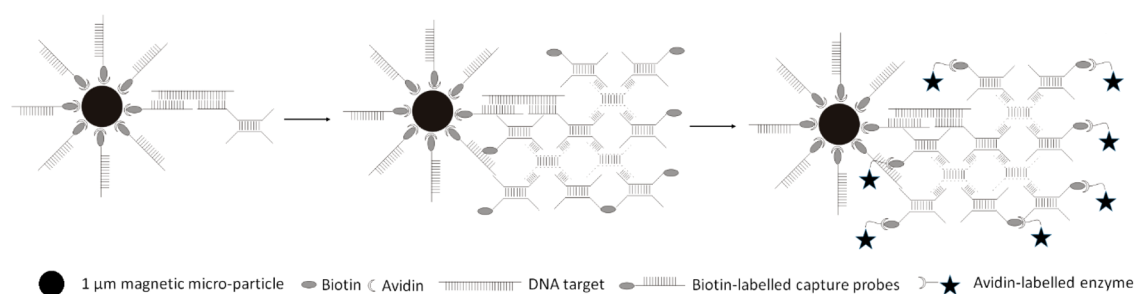


**Figure 3.** Schematic representation of db DNA-based ELISA. The target DNA is anchored to the magnetic microparticles (MMPs) by the biotin-labeled capture probes and then recognized and amplified by the biotin-labeled db DNA units. The enzyme is linked to the complex through the interaction between enzyme-decorated avidin and biotin reaction.

simple washing step, implemented as cycles involving the addition of one primer (followed by incubation, washing and then addition of the second primer in a new cycle). At each cycle, the number of exposed sticky ends created is 3 per primer bound, the number of which is linked to the number of sticky ends at the previous cycle. The size of the structure thus scales in a controlled and well-defined manner as  $4 \times 3^n$  db DNA primers, where  $n$  is the number of cycles (Figure S2).

The washing steps can be conveniently performed, using a magnetic microbead solid support (Figure 2), taking advantage of their high surface-to-volume ratio (as previously demonstrated through the host of applications they have been used in, such as biobarcode,<sup>12</sup> DNA-based fluorescence nanobarcodes,<sup>13</sup> and enzyme based optical nanoprobos).<sup>14</sup> Here, we attached a biotin-labeled DNA capture probe on the surface of a microparticle through an avidin coupling as previously described.<sup>13</sup> The probe was complementary to a target DNA sequence (the analyte to be detected), which was then bound onto the bead. One sticky end of a db DNA primer was designed to be complementary to the target DNA sequence, such that it can initiate the amplification reaction and hybridize with the target DNA on the bead. The first primer was washed off and replaced by the second db DNA primer. Three molecules hybridize to the first primer, and the reaction can then be cycled to achieve signal amplification. To detect the

hybridization and thus the target DNA sequence, both primers were labeled with the fluorophore Cy5 at their 5' stick ends (two fluorophore per primer). Theoretically (Figure 1a), the number of fluorophore in the construct thus should increase by a factor  $3^n$ , potentially yielding a large signal for a small number of target molecules bound toward single molecule detection.

To confirm the mechanism proposed, we captured super-resolution images of individual beads as the rational HCR progresses. The number of captured fluorescence-labeled db DNA units on the surface of the microbeads increases (Figure 2a) for each cycle, leading to an exponential amplification of the fluorescence signals that started from individual immobilized targets as shown by the super-resolution images presented and quantified in Figure 2b. The size of the fluorescent clusters, identified by segmentation (see Figure S4 for an example of the process), increases as the beads are processed through more cycles of hybridization and wash. By increasing the target DNA concentration, the number of spots on each bead can increase significantly, indicating that each spotlike feature represents the signal of a single event (Figure S3). The signal can also be viewed using a normal fluorescence microscope (Figure S3).

**Assay Format.** As a practical demonstration, the detection of the sensing events at such low concentrations using fluorescence is not feasible routinely, as it requires scanning

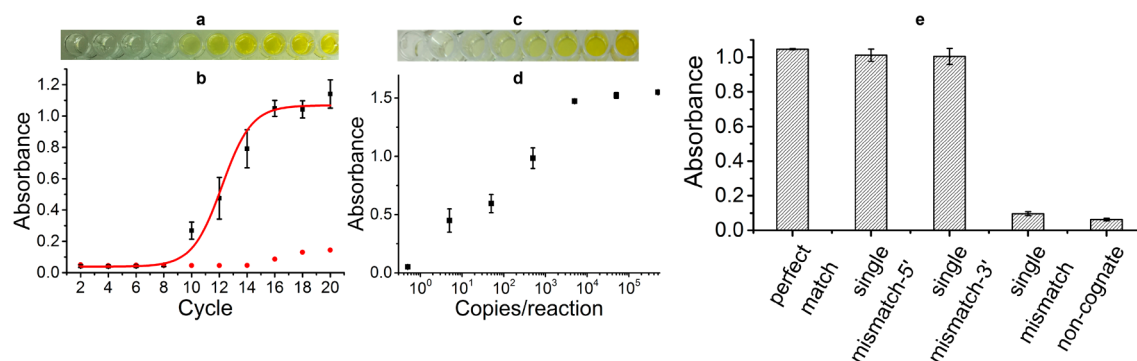


**Figure 4.** Rational enzyme-linked HCR. (a) Photograph indicates the color changing with different db DNA units addition times from 2 to 20 (cycles), respectively (left to right, target DNA concentration 5 pM), in a 96 microtiter plate. (b) Absorbance with respect to the blank was monitored at 450 nm. Black square: target concentration 5 pM. Red disk: ddH<sub>2</sub>O as a negative control. Data are the average of at least three replicates, and error bars represent the standard deviation. The data were fitted with nonlinear curve fitting to a Boltzmann curve ( $R^2 > 0.98$ ). (c) Analytical sensitivity. Color change with different target DNA concentration from 0.5 copies to  $5 \times 10^5$  copies/reaction (10 $\times$  increments per well) with the db DNA units addition times at 35 (cycles). The results are quantified in (d). Absorbance at 450 nm. Data are the average of at least three replicates, and error bars represent the standard deviation. The signal increases until a plateau is reached after 5000 copies/reaction. The limit of detection is 5 copies/reaction. (e) 1 pM of different target DNA molecules was added to the reaction: perfect match DNA, single mismatch DNA with the defect located at different position (toward the 5' end, the 3' end and in the middle respectively), and noncognate DNA. The sequences are provided in Table S1. Data are the average of at least three replicates, and error bars represent the standard deviation.

observation fields with high magnification to identify individual fluorescent beads. We thus adapted the signal amplification technique of enzyme-linked immunosorbent assays (ELISA),<sup>14,15</sup> where an avidin-labeled enzyme (horseradish peroxidase, HRP, ca. 6 nm in diameter) was attached to a biotin-db DNA primer (Figure 3). To avoid unspecific binding of the enzyme onto the bead surface, this was only added at the last cycle, at the end of the rational HCR. Two out of the three sticky ends of the db DNA primer host a biotin moiety. After cycle  $n$ , there are  $4 \times 3^n$  sticky ends, yielding  $8 \times 3^{n-1}$  sites for the immobilization of HRP, forming a densely packed HRP complex on the surface of the microbeads. The result of db DNA-based enzyme-linked HCR analysis was quantified on a microplate reader (450 nm) or directly by the naked eye (Figure 4), after the substrate (tetramethylbenzidine, TMB) was added.

The observed response curve is analogous to that of a real-time PCR assay, Figure 4a, with the signal increasing exponentially with the number of cycles performed, until kinetically depleted. We could define an equivalent cycle threshold (Ct) of 9 when the signal reaches a level of intensity higher than 3 standard deviation off the background. A linear regression of the logarithm of the absorbance in the exponential phase reveals a slope of  $0.25 \pm 0.03$ , which would correspond to an amplification factor of  $1.28^{n-1}$  (as opposed to  $3^{n-1}$ , predicted theoretically). We attribute this limitation in efficiency to two main factors, namely the fact the thermodynamic equilibrium of all DNA bound is kinetically limited, leading to unbound DNA, as well as steric hindrance, which limits DNA binding to available sites in complex, large structures together with HRP labeling in the final step.

The signal reached a plateau after cycle 16, when the number of molecules added at the beginning of the cycle (free db DNA primer 0.5  $\mu$ M, ca.  $10^{10}$  molecules) is of the same order as that of sticky ends present on the beads ( $8 \times 3^{15}$ , ca.  $10^9$ ), thus limiting the efficiency of the reaction (as discussed in Figure 1b).

**Analytical Performance.** The analytical performance of the assay, as shown in Figure 4c,d, shows a limit of detection of

five molecules in a 20  $\mu$ L reaction after 35 cycles. Once amplified, the signal was also detectable with the naked eye (Figure 4c). Specificity was evaluated using an excess of noncomplementary target DNA, which did not produce a significant absorption compared to specific target DNA (Figure 4e). Further, we also studied the ability of the assay to effectively discriminate a single-base mismatch in the target DNA (Figure 4e). The technique relies on DNA hybridization, and we observe behaviors similar to those of other techniques based on the same principle, such as DNA microarrays.<sup>16</sup> The discrimination is not effective when the defect is located at the edges of the binding sequence, but the probe sequence can be designed to yield a signal close to that of a noncognate DNA and provide excellent mismatch discrimination, when the defect is located in the middle of the sequence.

Contrary to DNA-based signal amplification methods developed previously, such as chemical cross-linked dendritic DNA,<sup>16–18</sup> DNA nanobarcode,<sup>13,19</sup> and backbone-branched oligonucleotides,<sup>20–22</sup> this rational HCR cycling method harnesses the level of control of biochemical reactions that has been instrumental in placing PCR as a gold standard technique in molecular biology. The microbead-based assay process is also simple and convenient, where analysis of a few copies of target DNA can be performed visually, with the naked eye, making it suitable for performing DNA-based diagnostics.

**Clinical Applicability.** To demonstrate the applicability of the technique in the clinic, we designed an assay to detect hepatitis B virus (HBV) in patients. HBV is a major cause of death worldwide (comparable to HIV and tuberculosis—1.46 millions death in 2013).<sup>23</sup> If the elimination targets (by 2030) of the World Health Organization are to be met, better approaches to reach underserved populations are to be developed. In a group of 54, our cyclic HCR methodology detected 37/38 infected patients (benchmarked against real-time qPCR), missing only one patient in the cohort, who had a low infection burden (<10 copies, see Figure 5 and data in the Supporting Information). There was very good agreement with

rt-qPCR, on par with the best assays available; see also Figure 5.

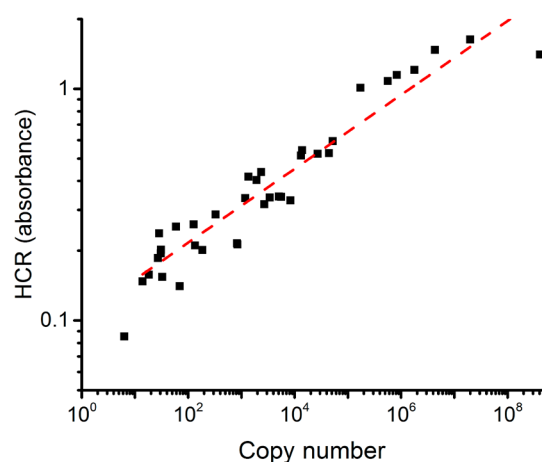


**Figure 5.** Correlation between the copy number of each clinical sample and the intensity of the signal (absorbance) obtained after rational 35 cycles of HCR. Dashed red line is a linear fit ( $R^2 = 0.9$ ). The lowest copy number sample was not detected using rational HCR (signal below threshold of 0.12).

## CONCLUSIONS

In this work, we have designed and demonstrated a cyclic HCR technique to detect DNA molecules using an enzyme-free amplification scheme. The control enabled by cycling the reaction, akin to that available in PCR, led to high sensitivity (ca. five copies). We also demonstrated the applicability of the method in clinical study to detect HBV in the serum of patients. The method could also in the future be used for single molecule sensing by using electrochemical detection for HRP-catalyzed reactions<sup>24</sup> or super-resolution microscopy as illustrated here. Furthermore, the db DNA primer units are both efficient structural scaffolds and functional molecules which could be modified to develop proteomic and metabolomic assays by replacing the target DNA with aptamers.<sup>25</sup>

## EXPERIMENTAL METHODS

**Oligonucleotides Designs.** The oligo sequences were designed and tested for hybrids and hairpin structures using the Integrated DNA Technologies design tools;<sup>26</sup> sequence information can be found in Table S1. The oligos were commercially synthesized, PAGE purified (Eurofins, UK), and dissolved in TE buffer (10 mM Tris, 1 mM ethylenediaminetetraacetic acid (EDTA), pH = 8.0) to a final concentration of 100  $\mu$ M. Two db DNA units were constructed by mixing two specific oligonucleotide components (1:1 molar ratio) in 2 $\times$  SSC buffer with a final concentration of 2  $\mu$ M for each oligonucleotide. The hybridizations were performed as follows: (1) denaturation at 95  $^{\circ}$ C for 5 min; (2) annealing at 50  $^{\circ}$ C for 10 min; (3) further annealing at 37  $^{\circ}$ C for 10 min. The final annealed products were stored at room temperature. The db DNA units were evaluated on 3% agarose gel in 0.5 $\times$  TBE buffer at 75 V for 2 h, stained with SYBR Gold Nucleic acid Gel Stain (Thermo Fisher Scientific) (lanes 1 and 2 in Figure 1b).

**Fluorescence Microscopy Imaging.** The conjugation of the magnetic microbeads and the DNA capture probe was carried out using a modified protocol (Bangs Laboratories) as previously described.<sup>13</sup> Briefly, 1.0  $\mu$ g of avidin-coated microparticle (5  $\mu$ m) suspension was washed with 100  $\mu$ L of TTL buffer (100 mM Tris-HCl, 0.01% Tween 20, 1 M LiCl, pH 8.0) and resuspended in 10  $\mu$ L

of TTL. A 1 pmol portion of biotin-modified capture DNA probe was then mixed with the resuspended microparticle solution and incubated at room temperature for 30 min with gentle agitation. The excess and weakly bound probes were then washed away using 100  $\mu$ L of TTL buffer, TT buffer (250 mM Tris-HCl, 0.01% Tween 20, pH 8.0), TTE buffer (250 mM Tris-HCl, 0.01% Tween 20, 20 mM Na<sub>2</sub>(EDTA), pH 8.0), and TT buffer after centrifugation at 5000g for 3 min. The capture probe functionalized microparticles were incubated at 68  $^{\circ}$ C for 30 min in a prehybridization buffer (0.5 M sodium phosphate, 1 mM EDTA, 7% (wt/vol) SDS and 1% (wt/vol) BSA (pH 8.0)) to functionalize the surface. After removing the prehybridization buffer, the probe-functionalized microparticles were resuspended and stored in hybridization 1  $\times$  SSC buffer.

The sample for fluorescence microscopy was prepared by thoroughly mixing the capture probe functionalized polystyrene microbeads suspension with target DNA in 50  $\mu$ L hybridization buffer at room temperature for 30 min to ensure uniform coating. Subsequently, 5  $\mu$ L of 1  $\mu$ M detection probe conjugated with U1 (formed with ssDNA U1-1' and U1-2) was added into the solution and incubated at room temperature for 30 min. U1 hybridized onto microbeads in the presence of target DNA via a sandwiched hybridization (Figure 2a). The sample was washed three times with 50  $\mu$ L of hybridization buffer to remove excess and weakly bound detection probe. The U1 immobilized microbeads were then mixed with formed Cy5-labeled U1 and U2 (5  $\mu$ L, 0.5  $\mu$ M) successively and repeatedly in 20  $\mu$ L hybridization buffer at room temperature for 20 min every time and centrifuged at 5000g for 3 min to remove the suspension. After that, the microbeads were washed with 50  $\mu$ L 0.2 $\times$  SSC buffer five times to remove excess and weakly bound db DNA units. The microbeads were concentrated to a final concentration of ca. 5000 beads/mL. A 1  $\mu$ L portion of the concentrated suspension was added onto a glass slide. A coverslip was glued onto the glass slide using nail varnish. For conventional fluorescence microscopy, the sample was imaged on a Zeiss LSM 800 confocal laser scanning microscope at 630-fold magnification using a far-red filter (Cy5). The images were analyzed using the ZEN 2.1 lite software. For super-resolution microscopy (STORM), the samples were imaged using an ELYRA PS1 microscope (Zeiss), using a 100 $\times$  Plan-apochromat objective (NA 1.46 oil immersion). A series of 2000 cycles were acquired in total internal reflection microscopy (TIRF) mode for each experimental measurements using 642 nm laser (100% power) and 405 nm laser (1% power during integration). For visualization, "Localization Precision" (20–35 nm) and "Chi Square" (1.5–3) filters were used. Images were segmented using CellProfiler (v2.2.0)<sup>27</sup> to identify fluorescent spots and measure shape and intensity.

**db DNA-Based ELISA.** For db DNA-based ELISA, the preparation of capture probe coated magnetic microparticles (MMPs) (Thermo Fisher Scientific) was carried out as previously described.<sup>14</sup> Briefly, the avidin modified MMPs (1  $\mu$ m) were washed with 100  $\mu$ L of washing buffer (50 mM Tris-HCl, 150 mM NaCl, 0.05% Tween 20, pH 8.0) twice. A solution of biotinylated capture probe was added to the collected MMPs (at a ratio of 2.5 nmol probe 1 to 1 mg MMPs). The mixture was incubated at room temperature for 20 min with gentle shaking to immobilize the capture probe. The capture probe coated MMPs were collected using a magnetic separator, washed three times with washing buffer, and resuspended in blocking solution (10 mM phosphate sodium buffer solution, pH 7.4, 100 mM NaCl, 5% PEG and 2% BSA). After incubation at room temperature for 30 min, the treated MMPs were washed with washing buffer twice and stored in stocking solution (10 mM phosphate sodium buffer solution, pH 7.4, 100 mM NaCl and 1% BSA) at 4  $^{\circ}$ C until needed.

The samples for db DNA-based ELISA were prepared by mixing capture probe functionalized MMPs with target DNA in 50  $\mu$ L of hybridization buffer (5 $\times$  SSC, 0.05% Tween 20) at room temperature for 30 min to ensure uniform coating. A 5  $\mu$ L portion of 1  $\mu$ M detection probe conjugated with U1 (formed with ssDNA U1-1' and U1-2) was added into the solution and incubated at room temperature for 30 min. The sample was washed with 50  $\mu$ L of hybridization buffer three times to remove excess and weakly bound

detection probe. Then the U1 immobilized MMPs was mixed with U1 and U2 (5  $\mu\text{L}$ , 0.5  $\mu\text{M}$ ) successively and repeatedly in 20  $\mu\text{L}$  of hybridization buffer at room temperature for 20 min every time and collected using a magnetic separator. After addition of the db DNA units for 20 times in total (the last time was biotin-labeled U2 (5  $\mu\text{L}$ , 1  $\mu\text{M}$ )), MMPs were rinsed with washing buffer twice again and mixed with avidin–horseradish peroxidase (HRP) (Sigma) (20  $\mu\text{g}/\text{mL}$ ) in 50  $\mu\text{L}$  of 1 $\times$  PBS buffer for at 37  $^{\circ}\text{C}$  30 min. After being rinsed with 50  $\mu\text{L}$  of washing buffer seven times to remove the unbound avidin-HRP, 100  $\mu\text{L}$  of substrate solution containing TMB (Sigma) was added and mixed thoroughly and the mixture incubated at room temperature for 10 min before addition of 50  $\mu\text{L}$  of stop solution (1 M  $\text{H}_3\text{PO}_4$ , Sigma). The magnetic beads were removed using a magnetic separator, and the solution was moved to the 96-well plate for analysis using a microplate reader at 450 nm.

**Ethical Statement.** All procedures performed in studies involving human participants were in accordance with the ethical standards of the institutional and/or national research committee and with the 1964 Helsinki declaration and its later amendments or comparable ethical standards. All procedures were carried out in accordance with the “Measures on Ethical Review over Biomedical Research Involving Human Subjects” (Ministry of Health, China, January 11, 2007). All the samples were collected from patients after obtaining informed consent, and the data from these patients were used in this study only.

**Clinical Samples.** Fifty-four clinical samples were collected in March 2018 from Adicon Clinical Laboratories (Hangzhou, China). DNA was extracted from 200  $\mu\text{L}$  of serum using a magnetic beads-based method according to the provided instructions from the kit (Sansure Biotech, China). The extracted HBV-DNA was characterized with a quantitative PCR diagnostic kit (Sansure Biotech, Changsha, China) on an ABI 7500 real-time PCR system (2 min at 95  $^{\circ}\text{C}$ , followed by 45 cycles at 95  $^{\circ}\text{C}$  for 10 s and 60  $^{\circ}\text{C}$  for 30 s). Positive results were defined according to the instruction supplied. The sensitivity of the kit is 20 copies per reaction according to the instructions.

The hybridization process for HBV DNA detection included the following steps: 200  $\mu\text{L}$  of serum was used for HBV DNA extraction using the magnetic beads, and DNA was eluted with 20  $\mu\text{L}$  of 0.1 TE. The DNA was then denatured at 95  $^{\circ}\text{C}$  for 5 min to produce single-strand DNA; the solution was cooled to 50  $^{\circ}\text{C}$  and mixed with 20  $\mu\text{L}$  of probe-functionalized microparticles for 30 min, followed by two washes with 50  $\mu\text{L}$  of PBS on a magnetic rack. The detection probe conjugated with U1 (formed with ssDNA U1–1' and U1–2) was added into the solution and incubated at room temperature for 30 min. The hybridization process was repeated for 35 cycles. The data for each sample are available in the [Supporting Information](#). The capture probe and detection probe sequences were designed following previous research.<sup>28</sup> The threshold of each individual rational HCR assay was used to define the limit of detection with respect to the negative controls and was established as three standard deviations above the average signal for all negative samples (0.121). Extrapolating the linear fit of [Figure 5](#) to that threshold provides a theoretical limit of detection of three copies, below the experimental limit, which is between 6 and 14.

## ASSOCIATED CONTENT

### Supporting Information

The Supporting Information is available free of charge on the [ACS Publications website](#) at DOI: [10.1021/acsnano.8b03183](https://doi.org/10.1021/acsnano.8b03183). All data associated with this manuscript is available at <http://dx.doi.org/10.5525/gla.researchdata.632>.

Supplementary figures Table S1 ([PDF](#))

qPCR and cyclic HCR data ([PDF](#))

## AUTHOR INFORMATION

### Corresponding Author

\*E-mail: [jon.cooper@glasgow.ac.uk](mailto:jon.cooper@glasgow.ac.uk).

## ORCID

Julien Reboud: [0000-0002-6879-8405](https://orcid.org/0000-0002-6879-8405)

Jonathan M. Cooper: [0000-0002-2358-1050](https://orcid.org/0000-0002-2358-1050)

## Present Address

<sup>§</sup>(H.Z.) Laboratoire de Chimie des Polymères Organiques, LCPO, Université de Bordeaux, CNRS, Bordeaux INP, UMR 5629, 16 Avenue Pey Berland, 33600 Pessac, France.

## Notes

The authors declare no competing financial interest.

## ACKNOWLEDGMENTS

We are thankful to Dr. Leandro Lemgruber Soares (University of Glasgow) for super-resolution imaging. The work was supported by EPSRC (EP/I017887/1 and EP/K027611/1) and ERC 340117.

## REFERENCES

- (1) Vollmer, F.; Arnold, S. Whispering-Gallery-Mode Biosensing: Label-Free Detection down to Single Molecules. *Nat. Methods* **2008**, *5*, 591–596.
- (2) Notomi, T.; Okayama, H.; Masubuchi, H.; Yonekawa, T.; Watanabe, K.; Amino, N.; Hase, T. Loop-Mediated Isothermal Amplification of DNA. *Nucleic Acids Res.* **2000**, *28*, 63–63.
- (3) Xu, G.; Hu, L.; Zhong, H.; Wang, H.; Yusa, S.; Weiss, T. C.; Romaniuk, P. J.; Pickerill, S.; You, Q. Cross Priming Amplification: Mechanism and Optimization for Isothermal DNA Amplification. *Sci. Rep.* **2012**, *2*, 246.
- (4) Dirks, R. M.; Pierce, N. A. Triggered Amplification by Hybridization Chain Reaction. *Proc. Natl. Acad. Sci. U. S. A.* **2004**, *101*, 15275–15278.
- (5) Choi, H. M. T.; Beck, V. A.; Pierce, N. A. Next-Generation *In Situ* Hybridization Chain Reaction: Higher Gain, Lower Cost, Greater Durability. *ACS Nano* **2014**, *8*, 4284–4294.
- (6) Venkataraman, S.; Dirks, R. M.; Rothmund, P. W. K.; Winfree, E.; Pierce, N. A. An Autonomous Polymerization Motor Powered by DNA Hybridization. *Nat. Nanotechnol.* **2007**, *2*, 490–494.
- (7) Huang, J.; Wu, Y.; Chen, Y.; Zhu, Z.; Yang, X.; Yang, C. J.; Wang, K.; Tan, W. Pyrene-Excimer Probes Based on the Hybridization Chain Reaction for the Detection of Nucleic Acids in Complex Biological Fluids. *Angew. Chem., Int. Ed.* **2011**, *50*, 401–404.
- (8) Choi, H. M.; Chang, J. Y.; Trinh, L. A.; Padilla, J. E.; Fraser, S. E.; Pierce, N. A. Programmable *In Situ* Amplification for Multiplexed Imaging of mRNA Expression. *Nat. Biotechnol.* **2010**, *28*, 1208–1212.
- (9) Niu, S.; Jiang, Y.; Zhang, S. Fluorescence Detection for DNA Using Hybridization Chain Reaction with Enzyme-Amplification. *Chem. Commun.* **2010**, *46*, 3089–3091.
- (10) Saiki, R. K.; Gelfand, D. H.; Stoffel, S.; Scharf, S. J.; Higuchi, R.; Horn, G. T.; Mullis, K. B.; Erlich, H. A. Primer-Directed Enzymatic Amplification of DNA with a Thermostable DNA Polymerase. *Science* **1988**, *239*, 487–491.
- (11) Pfaffl, M. W.; Horgan, G. W.; Dempfle, L. Relative Expression Software Tool (REST©) for Group-Wise Comparison and Statistical Analysis of Relative Expression Results in Real-Time PCR. *Nucleic Acids Res.* **2002**, *30*, 36–36.
- (12) Nam, J.-M.; Thaxton, C. S.; Mirkin, C. A. Nanoparticle-Based Bio-Bar Codes for the Ultrasensitive Detection of Proteins. *Science* **2003**, *301*, 1884.
- (13) Li, Y.; Cu, Y. T. H.; Luo, D. Multiplexed Detection of Pathogen DNA with DNA-Based Fluorescence Nanobarcodes. *Nat. Biotechnol.* **2005**, *23*, 885–889.
- (14) Li, J.; Song, S.; Liu, X.; Wang, L.; Pan, D.; Huang, Q.; Zhao, Y.; Fan, C. Enzyme-Based Multi-Component Optical Nanoprobes for Sequence-Specific Detection of DNA Hybridization. *Adv. Mater.* **2008**, *20*, 497–500.
- (15) Li, J.; Song, S.; Li, D.; Su, Y.; Huang, Q.; Zhao, Y.; Fan, C. Multi-Functional Crosslinked Au Nanoaggregates for the Amplified Optical DNA Detection. *Biosens. Bioelectron.* **2009**, *24*, 3311–3315.

(16) Rennie, C.; Noyes, H. A.; Kemp, S. J.; Hulme, H.; Brass, A.; Hoyle, D. C. Strong Position-Dependent Effects of Sequence Mismatches on Signal Ratios Measured Using Long Oligonucleotide Microarrays. *BMC Genomics* **2008**, *9*, 317.

(17) Wang, J.; Jiang, M.; Nilsen, T. W.; Getts, R. C. Dendritic Nucleic Acid Probes for DNA Biosensors. *J. Am. Chem. Soc.* **1998**, *120*, 8281–8282.

(18) Capaldi, S.; Getts, R. C.; Jayasena, S. D. Signal Amplification through Nucleotide Extension and Excision on a Dendritic DNA Platform. *Nucleic Acids Res.* **2000**, *28*, 21–21.

(19) Lee, J. B.; Roh, Y. H.; Um, S. H.; Funabashi, H.; Cheng, W.; Cha, J. J.; Kiatwuthinon, P.; Muller, D. A.; Luo, D. Multifunctional Nanoarchitectures from DNA-Based ABC Monomers. *Nat. Nanotechnol.* **2009**, *4*, 430–436.

(20) Stoeva, S. I.; Lee, J.-S.; Thaxton, C. S.; Mirkin, C. A. Multiplexed DNA Detection with Biobarcode Nanoparticle Probes. *Angew. Chem.* **2006**, *118*, 3381–3384.

(21) Shchepinov, M. S.; Udalova, I. A.; Bridgman, A. J.; Southern, E. M. Oligonucleotide Dendrimers: Synthesis and Use as Polylabelled DNA Probes. *Nucleic Acids Res.* **1997**, *25*, 4447–4454.

(22) Shchepinov, M. S.; Mir, K. U.; Elder, J. K.; Frank-Kamenetskii, M. D.; Southern, E. M. Oligonucleotide Dendrimers: Stable Nanostructures. *Nucleic Acids Res.* **1999**, *27*, 3035–3041.

(23) World Health Organization. Combating hepatitis B and C to reach elimination by 2030. <http://www.who.int/hepatitis/publications/hep-elimination-by-2030-brief/en/> (accessed Apr 5, 2018).

(24) Crumbliss, A. L.; Perine, S. C.; Stonehuerner, J.; Tubergen, K. R.; Zhao, J.; Henkens, R. W.; O'Daly, J. P. Colloidal Gold as a Biocompatible Immobilization Matrix Suitable for the Fabrication of Enzyme Electrodes by Electrodeposition. *Biotechnol. Bioeng.* **1992**, *40*, 483–490.

(25) Xiao, Y.; Lubin, A. A.; Heeger, A. J.; Plaxco, K. W. Label-free Electronic Detection of Thrombin in Blood Serum by Using an Aptamer-based Sensor. *Angew. Chem.* **2005**, *117*, 5592–5595.

(26) PrimerQuest program, IDT, Coralville, Iowa, USA. Accessed 12 December, 2018. <http://www.idtdna.com/SciTools>.

(27) Lamprecht, M. R.; Sabatini, D. M.; Carpenter, A. E. CellProfiler: Free, Versatile Software for Automated Biological Image Analysis. *BioTechniques* **2007**, *42*, 71–75.

(28) Chen, C.-C.; Lai, Z.-L.; Wang, G.-J.; Wu, C.-Y. Polymerase Chain Reaction-Free Detection of Hepatitis B Virus DNA Using a Nanostructured Impedance Biosensor. *Biosens. Bioelectron.* **2016**, *77*, 603–608.